J. Chem. Soc. Nigeria, Vol. 47, No. 6, pp 1242 - 1258 [2022]

MODIFICATION OF TERMITE MOUND SOIL USING PHOSPHORIC ACID FOR PHOTODEGRADATION OF METHYLENE BLUE DYE UNDER UV LIGHT IRRADIATION

L. A. Madaki*, H. Ibrahim, P. A. Ekwumemgbo and C. E. Gimba

Department of Chemistry, Ahmadu Bello University, Zaria, Nigeria
*Correspondent Author: lamis_madaki@yahoo.com +2348032334405

ABSTRACT

Termite mound was mined from the termite nest spotted at Ahmadu Bello University, Zaria Kaduna State, Nigeria. It was washed with deionized water and placed in an oven set at 60^{o}C for 6 hrs before crushing with an aggregate impact crusher and sieved into 0.075 μm mesh pore size. The sieved soil sample was tagged as unmodified-TMS (termite mound soil). The soil sample was modified using orthophosphoric acid (H_3PO_4) at different (5 %, 10 %, 15 %, and 20 %) concentrations. The modified and unmodified-TMS were characterized by the methods of scanning electronic microscope (SEM), transmission electron microscope (TEM), Electron diffractive X-ray (EDX), Brunauer–Emmett–Teller (BET), Fourier transform infrared (FTIR), thermogravimetric analyses (TGA), and Selected area electron diffraction (SAED), The photocatalytic activity of the unmodified-TMS, 5 % TMS-H_3PO_4, 10 % TMS-H_3PO_4 , 15 % TMS-H_3PO_4 , and 20 % TMS-H_3PO_4, were assessed by testing the degradation rate of Methylene Blue under ultraviolet light irradiation using optimum parameters (1.5 g/L, pH 11 & 75 mg/L). The results indicated that the samples exhibited the best photocatalytic activity at optimum parameters of catalyst dosage 1.5 g /L. pH 11 and 75 mg/L concentration of MB as evidenced by the highest methylene degradation rate of (88 %). The photocatalytic degradation of Methylene blue dye was found to obey first-order kinetics.

KEYWORDS: Termite mound Soil, Methylene Blue, photocatalytic degradation, UV irradiation, Unmodified-TMS.

INTRODUCTION

The pollution of water bodies by untreated methylene blue dye effluents discharged from industries has been recently associated with the shortage of clean water in the society [1, 2]. This is common in developing countries where a high volume of wastewater is released into the physical environments without effective and efficient management [3]. Since the menace posed by methylene blue dye in the physical environment, scientists have been on the search for ways to remediate the environment with respect to the elimination of methylene blue dye.

Different treatment methods, including biological methods use of enzymes and micro-organisms, chemical methods and physicochemical methods mostly adsorption, have been widely applied to eliminate dye from the environment [4]. The adsorption methods include, but are not limited to, the use of rice husk, cow dung, and biochar [5]. [6]. Synthetic dyes remain in the physical environment since most of them are difficult to biodegrade [7] and are not usually eliminated during the conventional water treatment processes and, as such, persist in the environment

ISSN 0795 - 22066

due to their high stability to temperature, light, water, and other substances including soap and detergents [8]. Consequently, the so-called treated water apparently becomes a threat to biotic components in the environment [9]. In addition, food, cosmetics and pharmaceuticals industries are not left behind in consuming a large quantity of methylene blue dye for their productions [10]. Also, with respect to plants, the presence of methylene blue has become a major challenge, such as growth inhibition, reduction of pigment, and protein content of microalgae Chlorella vulgaris and Spirulina platensis [11]. Thus, the negative effects associated with methylene blue dye-loaded wastewater warrant the need for effective removal prior to industrial discharge. SiO_2 nanoparticles has been employed extensively in catalysis, separation, and adsorption research because of its enormous surface area, consistent pore size distribution, stable chemical characteristics, and comparatively high mechanical strength [12, 13]. Termite nests have been discovered all over the world, and it has been discovered that they are rich in organic waste, silica, and minerals like iron and aluminum [14]. Mound-building termites form termite nests, which significantly alter the physicochemical characteristics and mineralogy of the soil [15]. Inorganic-organic hybrid materials with organic functional groups bonded to silica surfaces are versatile heterogeneous catalysts [16]. Advances in technology have resulted in the development of silica materials containing a variety of different functional groups that can be used as a catalyst in organic synthesis. Recent developments have made it possible to develop silica materials with multiple, distinct functional groups that can be used as a catalyst in organic synthesis. Recently, photocatalysis is attracting increased interest because of its chemical stability, recyclability, low costs, and non-toxic processing routes [17].

MATERIALS AND METHODS

All chemicals and reagents used were of analytical grade purchased from Merck, Germany and BDH, England.

Sample Collection and Preparation

Termite mound was mined from the termite nest spotted at Ahmadu Bello University, Zaria, Kaduna State Nigeria. Plant materials in the sample were removed and air-dried in the laboratory at room temperature. The sample was washed with deionized water and placed in an oven set at 60 ^{0}C for 6 hrs before crushing with an aggregate impact crusher, sieved into 0.075 μm mesh pore size. The sieved soil sample was tagged as TMS (termite mound soil).

Modification of the Termite Mound Soil Using orthophosphoric acid

Modification of the termite mound soil using phosphoric acid was carried out. Five grams (5 g) each of the TMS was modified by adding the soil in 250 Cm^3 of H_3PO_4 acid at different concentrations of (5 %, 10 %, 15 %, 20 %) in a

ISSN 0795 - 22066

round bottom flask for 24 hrs after this process, the mixture was filtered and dried at 110^0C for 6 hrs. The catalysts were then labelled 5 % TMS-H_3PO_4, 10 % TMS- H_3PO_4, 15 % TMS- H_3PO_4, and 20 % TMS- H_3PO_4.

Characterization of Catalyst

The morphologies and microstructures of the modified and unmodified catalysts were analyzed using a scanning electron microscopy (SEM) equipped with EDXA system, an X-ray diffraction (XRD) analyzer was used to characterize its crystallographic structure and crystallographic composition, The size, shapes, crystallinity and elemental analysis of the catalyst were carried out through transmission electron microscope (TEM). Selected area electron diffraction (SAED) pattern was recorded from TEM images to obtain the crystal structure. Joint Committee on Powder Diffraction Standards (JCPDS) software was then used to analyze the crystal planes. The FTIR spectrum of the synthesized catalyst was analyzed using a FTIR spectrometer (Thermo Fischer Scientific). The Brunauer–Emmett–Teller (BET) relationship was used to analyze the surface area and pore distribution. Thermal characterization of the catalyst samples was performed using Mettler-Toledo TGA/DSC

RESULTS AND DISCUSSION

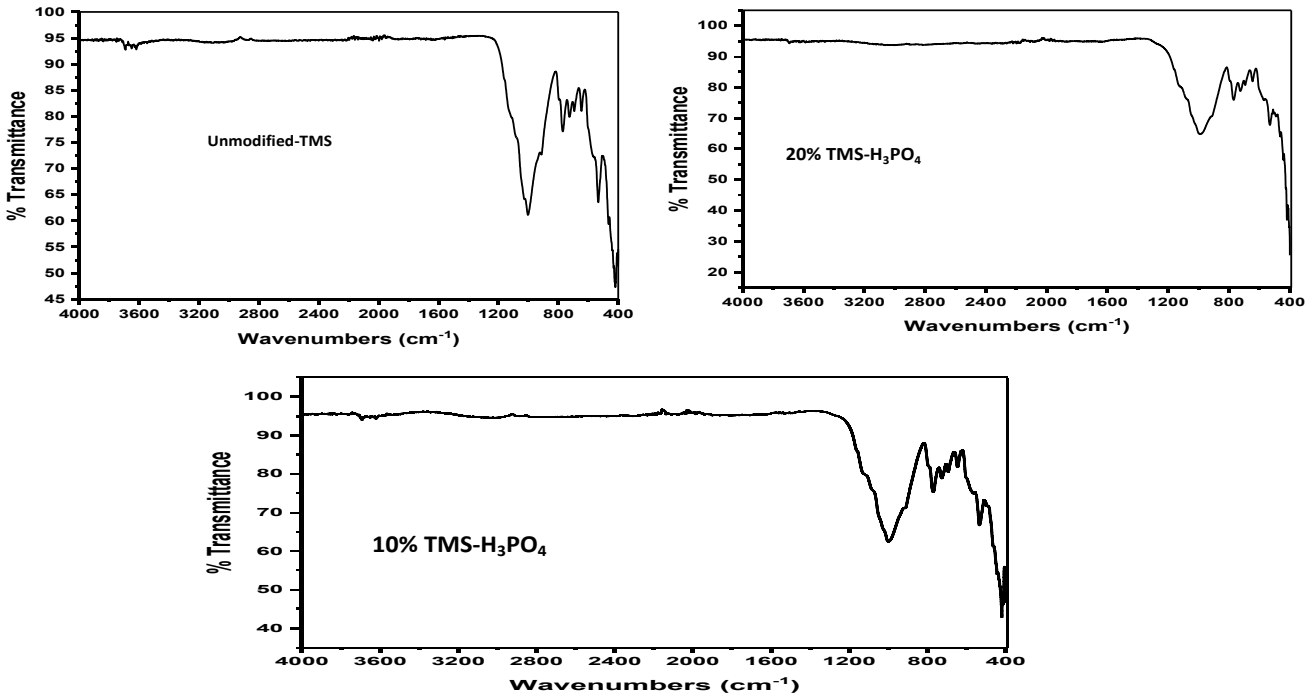

ISSN 0795 - 22066

Figure 1: FTIR (a) unmodified-TMS (b) 20 % TMS-H_3PO_4 and (C) 10 % TMS-H_3PO

FTIR Analysis

Figure (a) above shows the FTIR spectra of unmodified catalyst. The following absorption band were observed for the unmodified catalyst at 419, 534, 646, 726, 770 and 1003 cm^{-1} respectively. [18, 19]. The band at 1003 cm^{-1} is assigned to Si-O-Si bond stretching vibrations, the peaks at 726 and 770 cm^{-1} corresponds to O-H bending. Peaks at 646 cm^{-1} was due to Si-O-Si bending while the absorption band at 534 was presenter to be O-Si-O bending vibration, Similar results were also recorded by other researchers [20., 21]. After modification of the termite mound soil with phosphoric acid at 5, 10, 15 and 20 % acid concentration, the FTIR spectra of the modified catalyst presented in Figure (1b and 1c) showed all the bands present in the unmodified sample with additional bands observed at 769 cm^{-1} assigned to P-O-H bending, 419 cm^{-1} to the Si-O rocking, at 770 and 533 cm^{-1} can be attributed to the O-H bending and O-P-O, O- Si-O bending respectively.

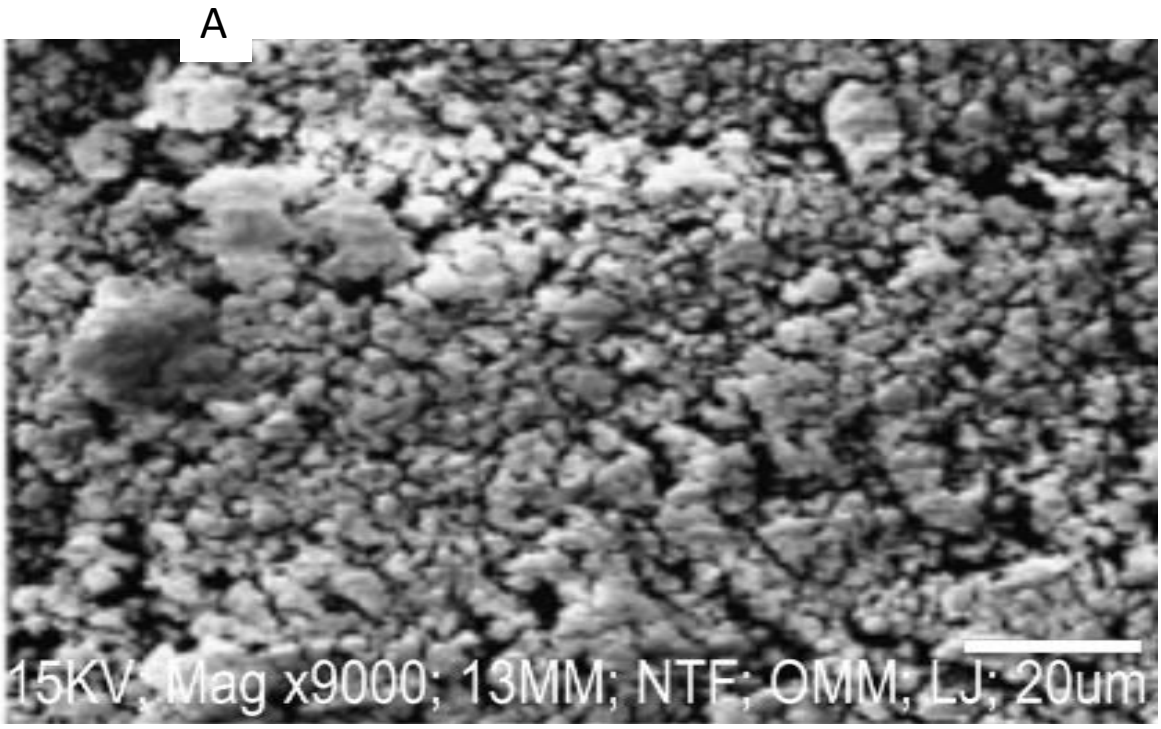

Scanning Electron Spectroscopy

ISSN 0795 - 22066

Plate 1: SEM images of Unmodified-TMS catalyst at different magnifications

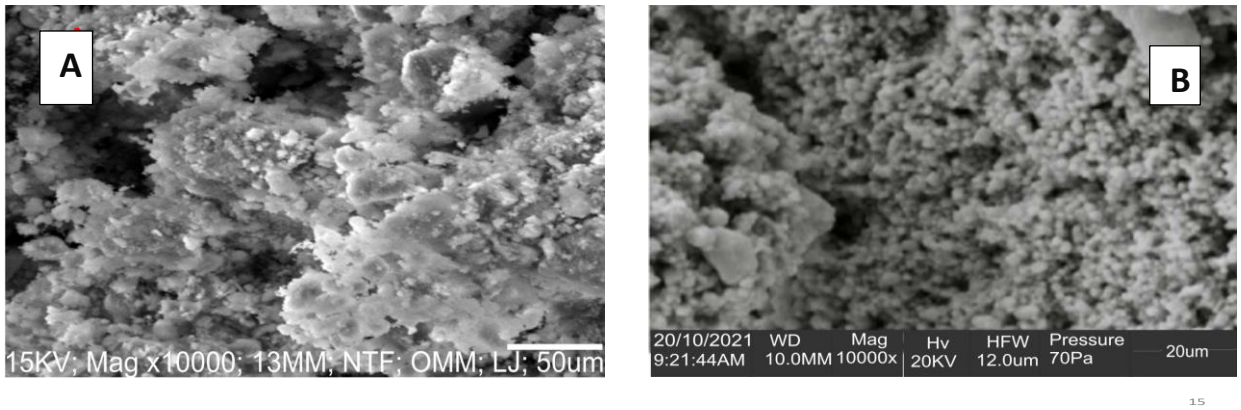

Plate 2: SEM (A) images of 20 % TMS- H_3PO_4 and (B) 10 % TMS-H_3PO_4 modified catalyst

The shape and surface morphology of the unmodified termite mound soil were further characterized by (SEM) as shown by the micrographs in plate (1). The unmodified-TMS was observed to show rough surfaces and cracks with irregular shapes, the bright areas as shown on the micrographs are due to thin layers of fine particles adhered to surfaces of the catalyst which is dominantly composed of quartz sand minerals [20]. Surface morphology for the 20 % TMS-H_3PO_4 catalyst was also observed by the scanning electron microscope (SEM) images as shown in Plate (2a). The images showed that the agglomerate of 20 % TMS- H_3PO_4 is widely dispersed. Mesoporous surface roughness and shape complexity of the catalyst is high in the case of 20 % TMS- H_3PO_4 as compared with the unmodified catalyst which resulted in a high surface area as observed by other authors [21, 19]. It was observed to be extremely rough nanocrystalline as seen in Plates (2a & 2b) composed of particles with heavy agglomerates. The dispersion of these catalysts improved significantly than the unmodified-TMS as shown in Plates (1a, b), the use of phosphoric acid at different concentrations for the modification must have eliminated some residual impurities from the surface of the catalyst such as heavy metals with high atomic numbers and aluminosilicate as also observed by [19]. A similar trend of spherical particles with heavy agglomerates was also observed for the 10 % TMS-H_3PO_4 catalyst as shown in Plate (2 b) above.

Transmission Electron Spectroscopy

The unmodified-TMS had a chain structure and were composed of primary spheres with a strong

ISSN 0795 - 22066

diameter of approximately 3.7 nm in the same aggregate plate (3). The aggregate shape is in principle like soot particles [26], but the surface of the catalyst was observed to be rough and there appears some non-uniformity in the shapes and sizes due to clustering of particles. SEM images for the unmodified termite mound soil as shown by the micrographs in Plate (3 a) also confirmed the rough surface of the catalyst and the appearance of some spherical shapes amidst irregularity in shapes.

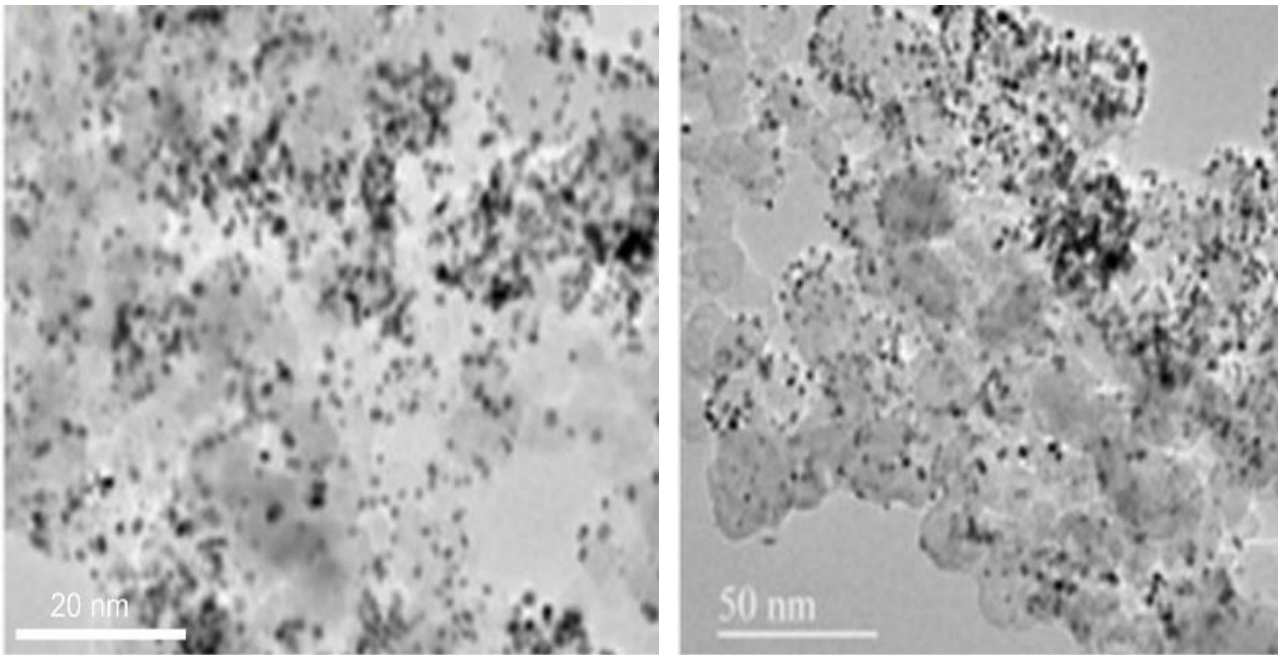

Plate 3: TEM images of Unmodified-TMS catalyst at different magnifications

ISSN 0795 - 22066

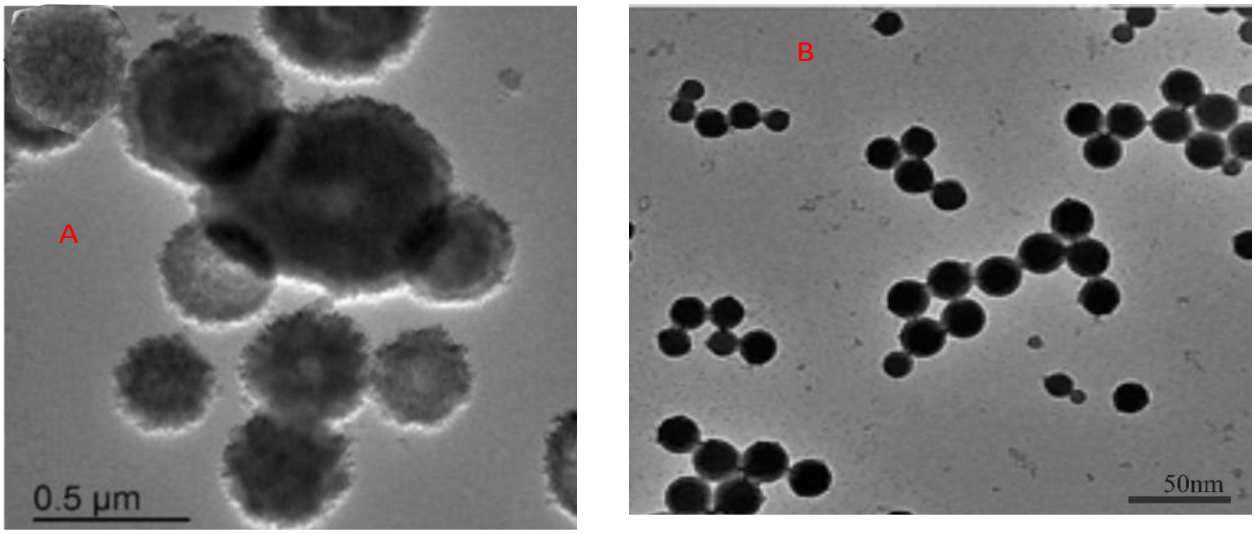

Plate 4: (a) TEM images of 20 % TMS-H_3PO_4 and (b) 10 % TMS-H_3PO_4 [18]

Plate (4a), shows a typical TEM images of the acid modified catalyst 20 % TMS-H_3PO_4 at different magnifications, the samples mostly consist of spherical like particles of different sizes packed in aggregate layers with variable diameter mostly ranging from approximately 326 nm – 409 nm in good agreement with the SEM micrographs. The modified 20 % TMS-H_3PO_4 catalyst showed good mono dispersion of the particles after modification with 20 % phosphoric acid. This is attributed to the presence of Bronsted acid sites SiO_2-PO_4 High monodispersed and spherical nanoparticles were observed on the micrograph of 10 % TMS- H_3PO_4 modified catalyst as shown in Plate (4b). These shows that dispersed spheres with a size of approximately 17.7 nm which is lesser than that obtained from the 20 % TMS- H_3PO_4 and higher than the unmodified termite mound soil.

ISSN 0795 - 22066

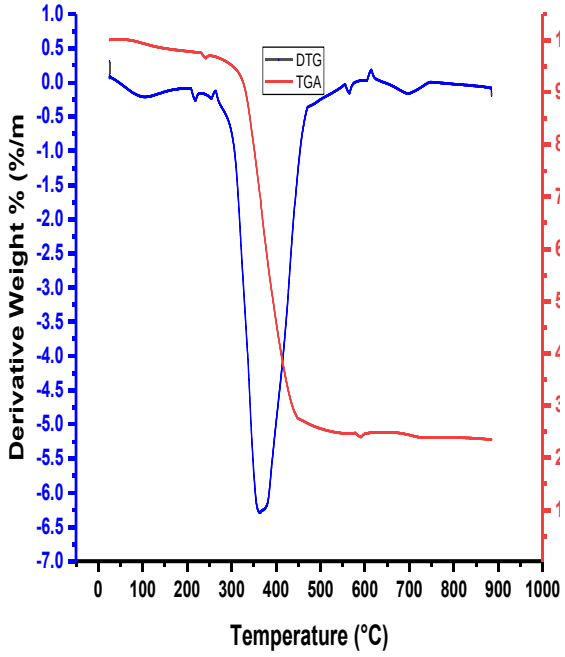

Figure 2:TGA-DTG for Unmodified-TMS

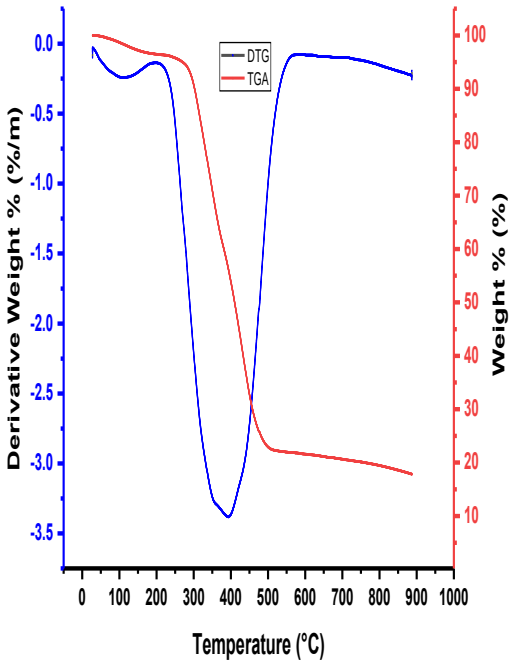

Figure 3: TGA-DTG 20 % TMS-H_3PO_4

The TGA result obtained for unmodified-TMS catalyst as shown on figure (2), the curve showed four steps weight loss respectively. The thermogram showed the first weight loss step of about 3.1 wt. % was observed in the range 102-243^{0}C attributed to desorption of surface water. The second step occurred between 243-320 ^{0}C with 3.3 wt. % loss corresponding to probably decomposition of organic content present in the modified catalyst, the major weight loss was observed to be 65.38 wt. % starting at 320- 442 ^{0}C probably due to decomposition. Fourth step was 5.02 wt. % loss at 442 - 711.6 ^{0}C which could be ascribed to carbonization of hydrocarbons compounds, the unmodified termite mound soil became stable at 884.9^{0}C with residual weight of 23.6 wt. %.

The 20 % TMS-H_3PO_4 catalyst was analyses using TGA the results obtained as shown on Figure (3) indicated a three weight loss steps as observed on the thermogram respectively. The first step occurred at less than 130 ^{0}C with 2.0 wt. % loss which might corresponds to the removal of water components, the second step occurred at the range of 130- 289 ^{0}C with 3.7 wt. % loss, this could be due to loss of low weight molecular compounds or first decomposition products. Major weight loss was observed to be 71.01 wt. % at 289.7- 491.4 ^{0}C which can be as a result of decomposition. At temperature of 491.4 - 886.35^{0}C range 5.27 wt. % loss was observed this can be related to carbonization of hydrocarbon compounds, the acid modified catalyst showed

ISSN 0795 - 22066

great stability and no further weight loss step was observed with 18.02 wt. % residue left.

SAED ANALYSIS

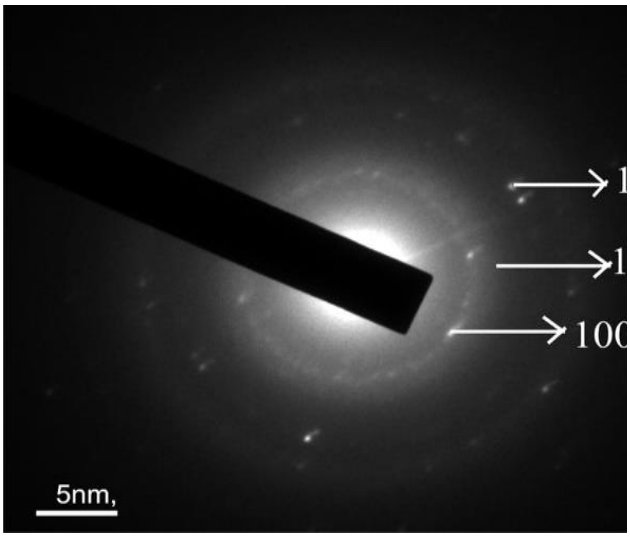

Plate 5: SAED pattern of Unmodified- TMS catalyst

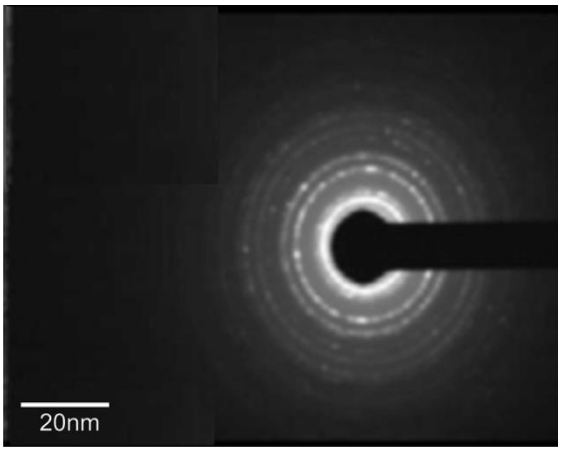

Plate 6: SAED pattern of 20 % TMS-H_3PO_4 modified catalyst

Selected area electron diffraction pattern of unmodified and acid modified termite mound catalyst is shown in Plate (5), and (6), The corresponding SAED for the Nano catalysts were observed. These rings are in agreement with the XRD spectra peaks, The images for all the catalysts confirms the poly and nanocrystalline nature of the samples due to the spot and ring patterns. The concentric rings with discrete spots in the SAED pattern indicate the polycrystalline nature and good crystallinity of the prepared catalyst. Also in agreement with the SAED results is the observed polycrystalline nature of the SEM images represented in Plate (2) The modified catalysts showed more crystallinity compared to the unmodified, these might be as a result of successful modification

Energy Dispersive X-ray Analysis

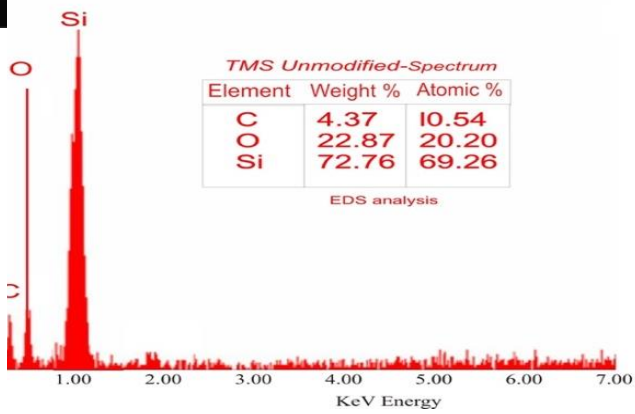

Figure 4: EDX Spectra of Unmodified TMS

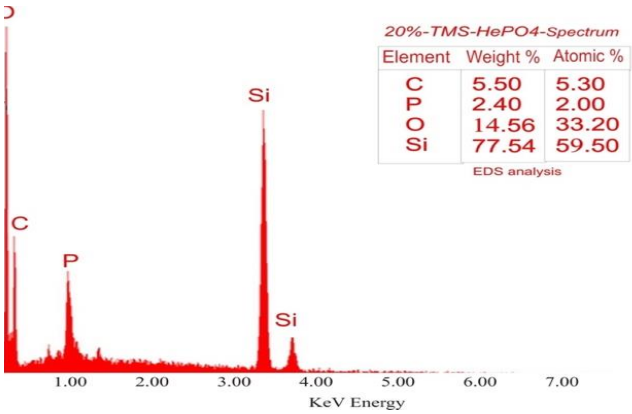

Figure 5: EDX 20 % TMS-H_3PO_4 Catalysts

ISSN 0795 - 22066

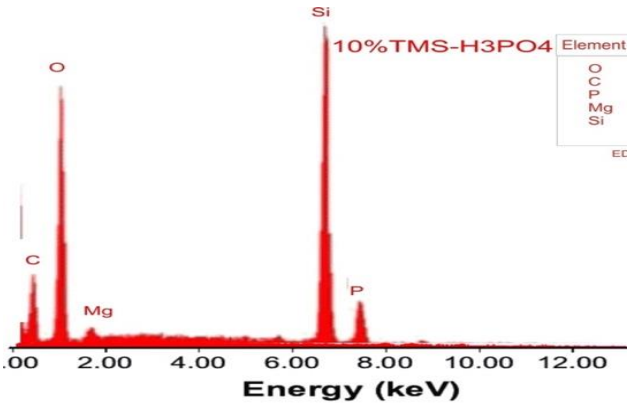

Figure 6: EDX 10 % TMS-H_3PO_4 Catalysts

The energy dispersive X-ray analysis was investigated in the binding energy region of 0-7 KeV as shown in Figure (4) for unmodified termite soil respectively. The EDX spectrum reveals the presence of two Intense peaks around 0.50 and 1.0 KeV assigned to the SiO_2 nanoparticles in the EDX spectra, the recorded peaks in regions 0.25, 0.5 and 1.0 KeV are related to C, O and Si binding energies indicating the presence of silica particles. The unmodified-TMS contains predominantly the elements Si and O which is also reveal by other authors [20]. Figure (5) above, showed the 20 % TMS-H_3PO_4 catalyst contains 77.54 % Si, 14.56 wt. % of O, 5.5 wt.% of C, and 2.4 wt. % of phosphorous as can been seen clearly on the spectra recorded in the region 1.0 -7.0 KeV. The analysis confirms the presence of Silicon (Si) and Oxygen (O) compounds as the predominant elements in the catalyst, the modification of the catalyst using phosphoric acid was evident from the EDX results obtained showing the presence of phosphorous which was absent in the unmodified-TMS The modification with 10 % TMS-H_3PO_4 showed the adsorption of phosphorous was more on the surface of the catalyst as compared to the 20 % TMS-H_3PO_4. The modification with 10 % TMS-H_3PO_4 showed the adsorption of phosphorous was more on the surface of the catalyst as compared to the 20 % TMS-H_3PO_4.

Brunauer-Emmett-Teller of catalysts

BET of the unmodified and acid modified catalyst the surface areas were obtained as 187.1, and 1518 and m^2/g for unmodified-TMS and 20 % TMS-H_3PO are respectively. The pore volume and average pore diameter size of the catalysts unmodified-TMS and 20 % TMS-H_3PO_4 were (0.0922 Cc/g, 2.136 nm and 0.7495 Cc/g, 2.126 nm). 20 % TMS-H_3PO_4 has the highest surface area of 1518 m^2 g^{-1}, high pore volume 0.7495 Cc/g and small pore size of 2.126 nm signifying high surface area, high pore volume and small pore size for high photocatalytic efficiency. The average pore size of between 2 nm and 50 nm is mesopores, all the catalysts were observed to be mesoporous.

PHOTOCATALYTIC DEGRADATION OF MB DYE

ISSN 0795 - 22066

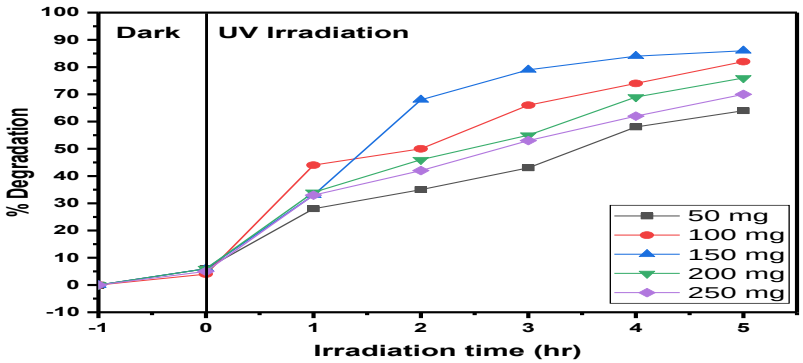

Figure 7: Effect of Catalyst Dosage using acid modified catalyst for MB Dye

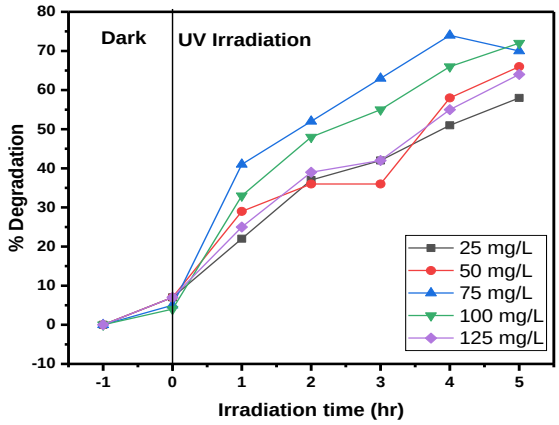

Figure. 8: Effect of concentration for degradation for MB Dye

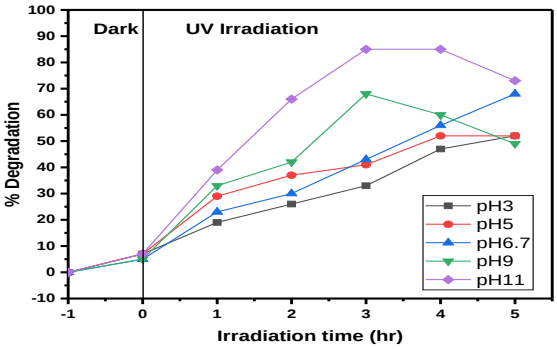

Figure. 9: Effect of pH for degradation of MB Dye

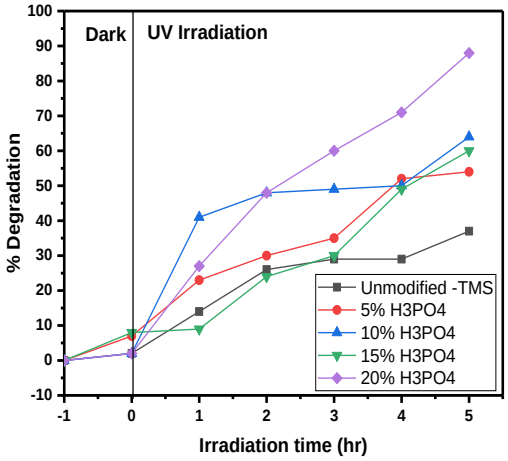

Figure. 10: Effect of catalyst Loading for MB Dye degradation

ISSN 0795 - 22066

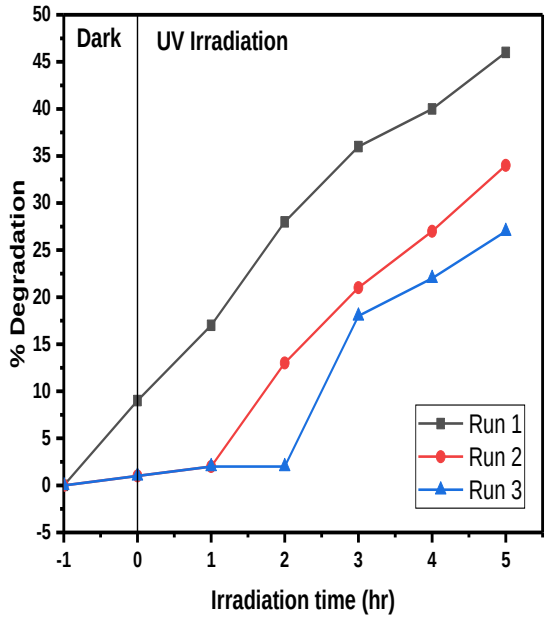

Figure 11: Reusability under UV Light Irradiation for MB Dye

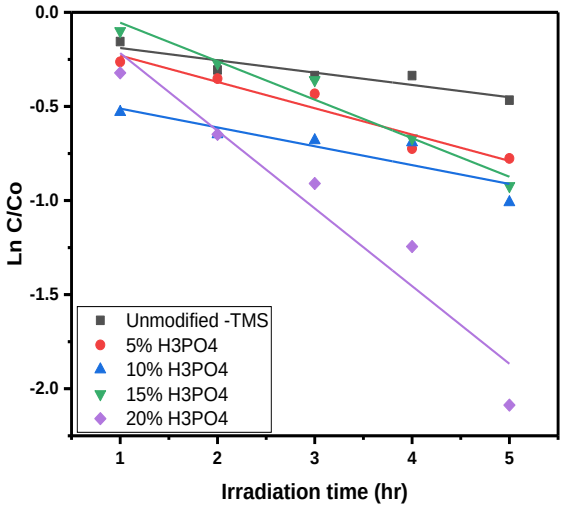

Figure 12:Pseudo first-Order kinetic model under UV light for MB

Table 1: Correlation Parameters of Pseudo First-Order Kinetic Model under UV Irradiation Using Acid Modified Catalyst for degradation

Catalyst	k (min^{-1})	R^2
Unmodified-TMS	0.0654	0.8178
5 % TMS-H_3PO_4	0.1399	0.9167
10 % TMS-H_3PO_4	0.1001	0.7189
15 % TMS-H_3PO_4	0.2047	0.9526
20 % TMS-H_3PO_4	0.4127	0.9115

Effect of Catalyst Dosage on Photo-Degradation of MB Dye Using UV Light

The effect of catalyst dosage on photodegradation efficiency presented in Figure (7) was analyzed by varying the catalyst dosage at a constant concentration of 125 mg/L of methylene blue solution and a pH of 6.698 respectively. Catalyst dosages of 50 mg, 100 mg, 150 mg, 200 mg, and 250 mg of 20 % TMS-H_3PO_4 modified catalyst were each added to 100 mL of 125 mg/L methylene blue solution, As observed in Figure 7, At the beginning, the photodegradation efficiency of methylene blue increased with increase in the amount of 20 % TMS-H_3PO_4 catalyst. Then, it decreased as the quantity of the catalyst increased continuously, caused by high turbidity in the reaction system and aggregation of the catalyst, [28]. The optimum additional amount of 20 % TMS-H_3PO_4 was 1.5 g/L as the value of the photodegradation efficiency for methylene blue

ISSN 0795 - 22066

reached 86 % after 300 min under ultraviolet light irradiation.

Effect of Initial Dye Concentration on The Degradation of MB Using UV Light

The degradation of Methylene blue dye at different initial concentrations of (25, 50, 75 100 and 125 mg/L) with a constant pH of 6.698 and a catalyst dosage of 1.5 g/L (20 % TMS-H_3PO_4). As shown in Figure (8), the maximum degradation of 74 % occurred for 75 mg/L of 20 % TMS-H_3PO_4 catalyst and 72 % was obtained for 100 mg/L of 20 % TMS-H_3PO_4 catalyst, this implies an increase in the concentration of dye decreases the percentage degradation. The equilibrium time for degradation was attained at 240 min. The degradation efficiency was to be inversely proportional to the increase in concentration, this is because as the dye concentration increases, the equilibrium adsorption of the dye on the catalyst active surface site increases, therefore resulting in the lower formation rate of $OH^{\cdot}$ radicals which is the principle oxidant in this process [29].

Effect of pH on the degradation of MB using UV light

Solution pH is known to be among the most significant variables influencing the degradation rate of dyes [30]. Thus, to study the influence of pH on the removal of MB, batch tests were performed at room temperature using 1.5 mg/L of catalyst dosage, 125 mg/L concentration of dye, and at different ambient pH values ranging from 3 to 11. The plot showing the effect of initial pH on MB dye degradation is illustrated in Figure (9). The observed degradation results at initial pH 3, 5, 6.7, 9, and 11 show that the degradation efficiency of methyl blue improved with an increase in pH. The maximum degradation was attained at pH 11. As observed in Figure (9), the amount of MB degraded at pH values of 3, 5, 6.7, 9, and 11 was 52, 52, 68, 68, and 85 %, respectively. Low solution pH values result in a positively charged surface that cannot provide hydroxyl groups for hydroxyl radical formation. Thus, the degradation efficiency of MB is lower under acidic pH. In contrast, higher pH values can instigate the formation of larger concentrations of ions (OH^-) that can react with the holes to form hydroxyl radicals ($^{\cdot}OH$), thereby enhancing the photodegradation of MB [30]. However, degradation of the dye is inhibited when the pH value is excessively high because the hydroxyl ions compete with the dye molecules for adsorption onto the surface of the photocatalyst, thereby reducing the adsorption of the dye molecule [31]. Also observed by other researchers. [32].

Effect of modified Catalysts on the degradation of MB dye using UV light

The effect of the different acid-modified catalysts on the photocatalytic degradation of Methylene blue dye was performed with optimal parameters of catalyst dosage 1.5 g/L, pH 11 and the methylene blue dye concentration of 75 mg/L. As shown in Figure (10). The MB degradation

ISSN 0795 - 22066

efficiency percentage was increased slightly with the increasing concentration of acid used for the soil modification. Photocatalytic degradation efficiency for all the catalysts was in the order Unmodified-TMS < 5 % TMS-H_3PO_4 < 15 % TMS-H_3PO_4 < 10 % TMS-H_3PO_4 < 20 % TMS-H_3PO_4 corresponding to 37 %, 54 %, 60 %, 64 %, and 88 % respectively. Modification of the termite mound soils with 5 %, 10 %, 15 % and 20 % orthophosphoric acid respectively, was observed to decrease the band gap energy when compared with the unmodified termite mound soil, also increasing in surface area of the catalyst after modification will improve the photocatalytic activity and increase the efficiency of photodegradation.

Reusability of 20 % TMS-H_3PO_4 catalyst under UV irradiation

The stability of the catalyst was determined by the efficiencies of the repeated degradation of (100 mL of 75 mg/L MB, the dosage was 1.5 g/L and pH 11 of 20 % TMS-H_3PO_4). The catalyst material was recovered by filtration and was washed several times with distilled water and subsequently dried at 60 °C for 12 h. The degradation efficiency of the recovered catalyst presented in Figure (11), showed that the degradation efficiency of MB reduced from 46.2% in the initial test to 27% after 3 cycles of testing. This may be due to a decrease in the surface-active sites of the catalyst or a mass loss of the catalyst during the recovery process.

Kinetic degradation study of the catalyst under UV light

The photocatalytic degradation of the Methylene blue dye was found to obey first-order kinetics at low dye concentrations. A plot of -ln C /C Vs irradiation time t, as shown in Figure (12). The linearity of the plot suggests that the photocatalytic degradation reaction approximately follows pseudo-first-order kinetics with rate constant (k_{app}) of 0.0654 min^{-1}, 0.1399 min^{-1}, 0.1001 min^{-1} 0.2047 min^{-1} and 0.4127 min^{-1} for Unmodified-TMS, 5 % TMS-H_3PO_4, 10 % TMS-H_3PO_4 15 % TMS-H_3PO_4, and 20 % TMS-H_3PO_4 photocatalyst, respectively.

CONCLUSION

Both acid and base modified catalysts exhibited improved photocatalytic activity compared to the unmodified-TMS. The order of photocatalytic performance for the acid modified catalysts : Unmodified-TMS < 5 % TMS-H_3PO_4 < 15 % TMS-H_3PO_4 < 10 % TMS-H_3PO_4 < 20 % TMS-H_3PO_4 UV-Visible irradiation, 10 % TMS-H_3PO_4 performed better than the 15 % TMS-H_3PO_4 this might be due to larger surface area, uniform pore size observed from the BET results, SEM images and possibly greater stability as shown by TGA/DTA results. All the acid modified catalysts exhibited improved photocatalytic activity with 20 % TMS-H_3PO_4 exhibiting the highest photocatalytic activity of (88 %) in ultraviolet

ISSN 0795 - 22066

irradiation The kinetic data for all the acid modified catalysts fit well with the pseudo first order kinetic model, the experimental results established that 20 % TMS-H_3PO_4 exhibited the highest photo-degradation rate constant (0.4127 min^{-1}) under UV.

REFERENCES

[1]. Hashem, A. H., Saied, E. & Hasanin, M. S., (2020). Green and ecofriendly bio-removal of methylene blue dye from aqueous solution using biologically activated banana peel waste. Sustainable Chemistry and Pharmacy,18,10033.https://doi.org/10.1016/j.scp.2020.100333.

[2]. Oladoye, P., Bamigboye, M., Ogunbiyi, O., & Akano, M., (2022). Groundwater for Sustainable Dev. Toxicity and decontamination strategies of Congo red dye. Groundwater Sustain Dev 19,100844. https://doi.org/10.1016/j.gsd.2022.100844.

[3]. Fito, J., Abrham, S. & Angassa, K. (2020). Adsorption of Methylene Blue from Textile Industrial Wastewater onto Activated Carbon of Parthenium International Journal of Environmental Research, 14, 501-511. doi:10.1007/s41742-020-00273-2

[4]. Cheng, J., Zhan, C., Wu, J., Cui, Z., Si, J., Wang, Q., Peng, X. & Turng, L.-S. (2020). Highly Efficient Removal of Methylene Blue Dye from an Aqueous Solution Using Cellulose Acetate Nanofibrous Membranes Modified by Polydopamine. ACS Omega, 5, 5389-5400.doi:10.1021/acsomega.9b0445

[5]. Ahmad, A., Khan, N., Giri, B. S., Chowdhary, P. & Chaturvedi, P. (2020). Removal of methylene blue dye using rice husk, cow dung and sludge biochar: Characterization, application, and kinetic studies. Bioresource Technology, 306, 123202.https://doi.org/10.1016/j.biortech.2020.123202

[6]. Liu, X.-J., Li, M.-F. & Singh, S. K. (2021). Manganese-modified lignin biochar as adsorbent for removal of methylene blue. Journal of Materials Research and Technology, 12, 1434-1445.https://doi.org/10.1016/j.jmrt.2021.03.076.

[7]. Cheng, J., Zhan, C., Wu, J., Cui, Z., Si, J., Wang, Q., Peng, X. & Turng, L.-S. (2020). Highly Efficient Removal of Methylene Blue Dye from an Aqueous Solution Using Cellulose Acetate Nanofibrous Membranes Modified by Polydopamine. ACS Omega, 5, 5389-5400.doi:10.1021/acsomega.9b0445

[8]. Rodríguez Couto, S. (2009). Dye removal by immobilized fungi. Biotechnology Advances,27,227-235. https://doi.org/10.1016/j.biotechadv.2008.12.001.

[9]. Sharma, J., Sharma, S. & Soni, V. (2021a). Classification and impact of synthetic textile dyes on Aquatic Flora: A review. Regional Studies in Marine Science, 45, 101802. https://doi.org/10.1016/j.rsma.2021.101802.

[10]. Dardouri, S., & Sghaier, J., (2017). Adsorptive removal of methylene blue from aqueous solution using different agricultural wastes as adsorbents. Korean Journal of Chemical Engineering 34,

ISSN 0795 - 22066

10371043. https://doi.org/10.1007/s11814-017-0008-2.

[11]. Krishna Moorthy, A., Govindarajan Rathi, B., Shukla, S. P., Kumar, K. & Shree Bharti, V. (2021). Acute toxicity of textile dye Methylene blue on growth and metabolism of selected freshwater micro algae Environs Toxicology and Pharmacology, 82, 103552.https://doi.org/10.1016/j.etap.2020.103552.

[12]. Fang, Y., Lakey, P. S. J., Riahi, S., McDonald, A. T., Shrestha, M., Tobias, D. J., Shiraiw M., & Grassian, V. H. (2019). A molecular picture of surface interactions of organic compounds on prevalent indoor surfaces: Limonene adsorption on SiO_2. Chemical Science, 10(10), 2906.2914.https://doi.org/10.1039/C8SC05560B.

[13] Zhang, W., Zhang, Y., Yang, K., Yang, Y., Jia, J., & Guo, L. (2019). Photocatalytic Performance of SiO2/CNOs/TiO2 to Accelerate the Degradation of Rhodamine B under Visible Light. Nanomaterials, 9(12),1671.https://doi.org/10.3390/nano9121671

[14]. Jouquet, P., Airola, E., Guilleux, N., Harit, A., Chaudhary, E., Grellier, S., & Riotte, J., (2017a.) Abundance and impact on soil properties of cathedral and lenticular termite mounds in Southern Indian woodlands. Ecosystems 20, 769–780.

[15] Tuma, J., Frouz, J., Veselá, H., Křivohlavý, F., & Fayle, T. M. (2022). The impacts of tropical mound-building social insects on soil properties vary between taxa and with anthropogenic habitat changeApplied Soil Ecology, 179, 104576

[16]. Wen, D., Li, W., Lv, J., Qiang, Z., & Li, M., (2020). Methylene blue degradation by the VUV/UV persulfate process: Effect of pH on the roles of photolysis and oxidation. Journal of Hazardous Materials 391, 121855.

[17] Ahmad, M. S., Ab Rahim, M. H., Alqahtani, T. M., Witoon, T., Lim, J. W., & Cheng, C. K. (2021). A review on advances in green treatment of glycerol waste with a focus on electro-oxidation pathway. Chemosphere, 276,130128.

[18]. Ayanda, O. S., Amodu, O. S., Adubiaro, H., Olutona, G. O., Ebenezer, O. T., Nelana, S. M., & Naidoo, E. B. (2019). Effectiveness of termite hill as an economic adsorbent for the adsorption of alizarin red dye. Journal of Water Reuse and Desalination,9(1),83–93. https://doi.org/10.2166/wrd.2018.026

[19]. Elghniji, K., Virlan, C., Elaloui, E., & Pui, A. (2018). Synthesis, characterization of SiO_2 supported-industrial phosphoric acid catalyst for hydrolysis of $NaBH_4$ solution. Phosphorus, Sulfur, and Silicon and the Related Elements, 193(12), 806–821.https://doi.org/10.1080/10426507.2018.1515946.

[20]. Mahamat, A. A., LindaBih, N., Ayeni, O., Azikiwe Onwualu, P., Savastano, H., Jr., & Oluwole Soboyejo, W.,(2021).Development of Sustainable and Eco-Friendly Materials from Termite Hill Soil Stabilized with Cement for Low-Cost Housing in Chad. Building. https://doi.org/10.3390/buildings11030086

[21] Zhang, Y.R.; Zhang, W.K.; Yang, K.; Yang, Y.Q.; Jia, J.; Liang, Y.; & Guo, L.J. (2019). Carbon nano-onions (CNOs)/TiO_2 composite preparation and its photocatalytic performance under visible light irradiation. J. Environ. Eng. 2019, in press, dor:10.1061/(ASCE)EE.1943-7870.0001662

ISSN 0795 - 22066

[22]. Opafola OT, Adekunle AA, Badejo AA, & Adeosun OJ (2020) Potentials of bentonite enhanced termite mound soil for bottom lining in waste containment system. J Degrade Min Lands Manage 7(3):2185–2191.https://doi.org/10.15243/jdmim.2020.073.2185

[23] Zhang, Y.R.; Zhang, W.K.; Yang, K.; Yang, Y.Q.; Jia, J.; Liang, Y.; & Guo, L.J. (2019). Carbon nano-onions (CNOs)/TiO_2 composite preparation and its photocatalytic performance under visible light irradiation. J. Environ. Eng. 2019, in press, dor:10.1061/(ASCE)EE.1943-7870.0001662

[24]. Elghniji, K., Virlan, C., Elaloui, E., & Pui, A. (2018). Synthesis, characterization of SiO_2 supported-industrial phosphoric acid catalyst for hydrolysis of $NaBH_4$ solution. Phosphorus, Sulfur, and Silicon and the Related Elements, 193(12), 806–821.https://doi.org/10.1080/10426507.2018.1515946.

[25]. Elghniji, K., Virlan, C., Elaloui, E., & Pui, A. (2018b). Synthesis, characterization of SiO_2 supported-industrial phosphoric acid catalyst for hydrolysis of $NaBH_4$ solution. Phosphorus, Sulfur, and Silicon and the Related Elements, 193(12), 806–821.https://doi.org/10.1080/10426507.2018.1515946.

[26]. Weinbruch, S., Benker, N., Kandler, K., Schütze, K., Kling, K., Berlinger, B., Thomassen, Y., Drotikova, T., & Kallenborn, R. (2018). Source identification of individual soot agglomerates in Arctic air by transmission electron microscopy. Atmos. Environ.172,47–54. https://doi.org/10.1016/j.atmosenv.2017.10.033

[27]. Mahamat, A. A., LindaBih, N., Ayeni, O., Azikiwe Onwualu, P., Savastano, H., Jr., & Oluwole Soboyejo, W.,(2021).Development of Sustainable and Eco-Friendly Materials from Termite Hill Soil Stabilized with Cement for Low-Cost Housing in Chad. Building.https://doi.org/10.3390/buildings11030086

[28] Eyimegwu, P. N., Lartey, J. A., & Kim, J. H. (2019). Gold-nanoparticle-embedded poly (N-isopropylacrylamide) microparticles for selective quasi-homogeneous catalytic homocoupling reactions. ACS Applied Nano Materials, 2(9), 6057-6066.

[29]. Shelar, S. G., Mahajan, V. K., Patil, S. P., & Sonawane, G. H. (2020). Effect of doping parameters on photocatalytic degradation of methylene blue using Ag doped ZnO nanocatalyst. SN Applied Sciences, 2(5), 1-10.

[30] El-Sayed, E., Marwa E., & Mona A. E.,(2018)."Biosynthesis and characterization of zerovalent iron nanoparticles and its application in azo dye degradation." Indian Journal of Chemical Technology (IJCT) 24.5 (2018): 541-547.

[31] Joorabi, F. T., Kamali, M., & Sheibani, S. (2022). Effect of aqueous inorganic anions on the photocatalytic activity of CuO–Cu_2O nanocomposite on MB and MO dyes degradation. Materials Science in Semiconductor Processing, 139, 106335.

[32] Alkaykh S., Mbarek A., Elbashir E. A.,(2020). Photocatalytic degradation of methylene blue dye in aqueous solution by $MnTiO_3$ nanoparticles under sunlight irradiation.

ISSN 0795 - 22066